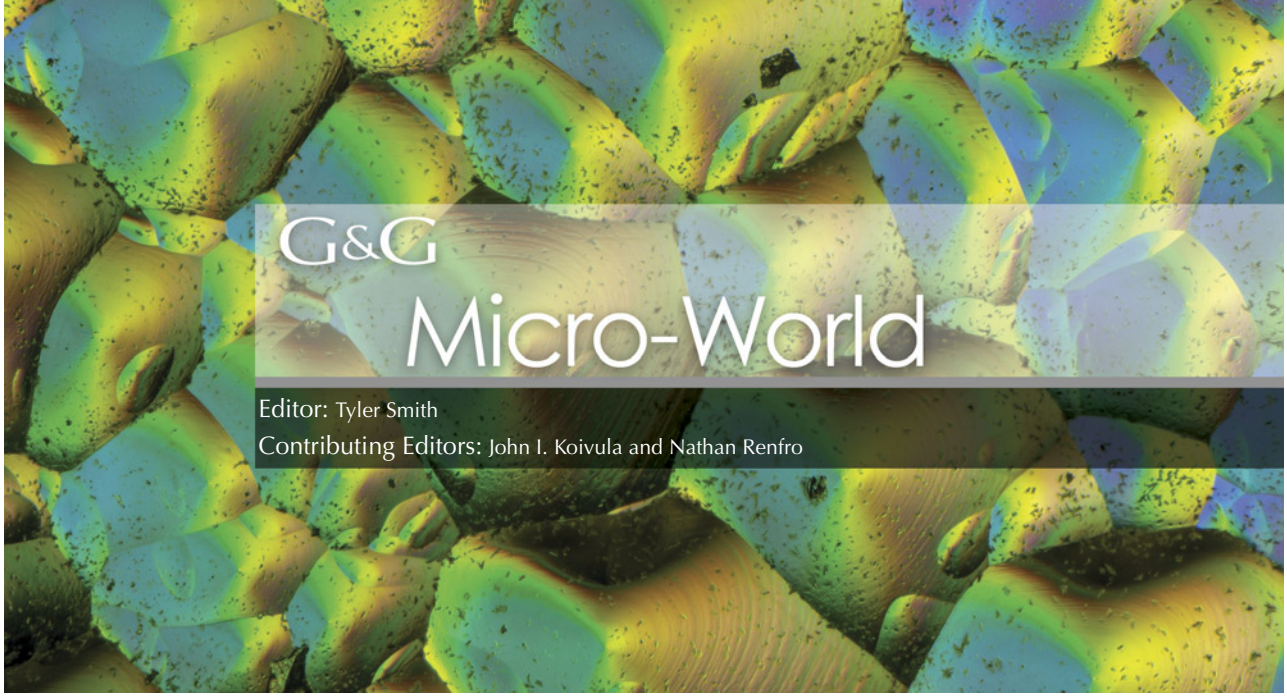

"Bamboo Forest" in Colombian Emerald

A recently examined 1.17 ct green stone exhibited dense tube inclusions running parallel to the *c*-axis (figure 1). The stone was identified as a Colombian emerald based on trace element chemistry measured by laser ablation–inductively coupled plasma–mass spectrometry analysis (S. Saeseaw et al., "Geographic origin determination of emerald," Winter 2019 *G&G*, pp. 614–646), and the profile was similar to that of samples from the Chivor district.

Long growth tubes are common inclusions in colored beryl-group gemstones that form in fluid-rich environments (e.g., Winter 2023 *G&G* Micro-World, p. 503; Fall 2024 Lab Notes, pp. 379–380). In this stone, the linear pavilion facet edges created the illusion of a corridor through a tranquil bamboo forest. The sawtooth graining occasionally observed in Colombian emeralds also was present, reminiscent of sunlight filtering through the bamboo. These impressions were enhanced as the emerald was imbued with a refreshing green color resulting from trace amounts of chromium and vanadium.

Taku Okada
GIA, Tokyo

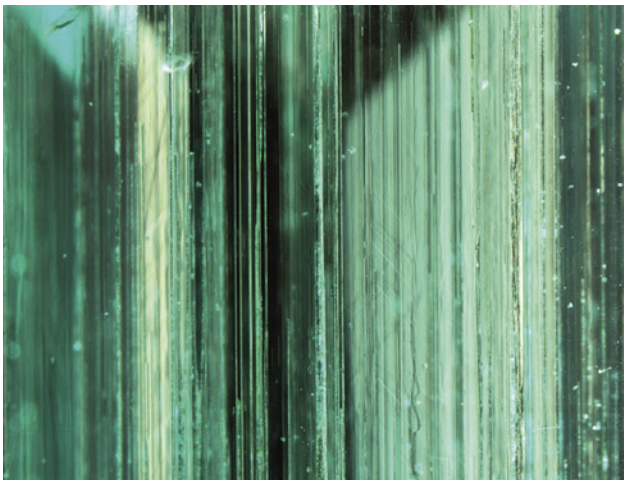

Figure 1. The effect of the pavilion facet edges on the dense tube inclusions in this Colombian emerald creates a scene reminiscent of a bamboo forest. Photomicrograph by Taku Okada; field of view 4.10 mm.

Blooming Bouquet: Thin Films in Russian Emerald

Some gems are enchanting both outside and in. Recently, the Lotus Gemology laboratory received an interesting submission of a 78.01 ct carved Russian emerald. According to the client, the emerald was carved by gemstone engraver Michael Peuster and inspired by art nouveau artist Alphonse Mucha. The woman depicted holds blooming flowers, symbolizing the arrival of spring (figure 2).

Microscopic examination revealed delicate, bouquet-like thin film inclusions on the back of the carving (figure 3). Iridescent thin films are frequently observed in emeralds from Russia, and this specimen showcased several striking

About the banner: Growth hillocks on the surface of this Russian laboratory-grown smoky quartz display vivid interference colors under polarized lighting. Photomicrograph by Nathan Renfro; field of view 10.02 mm. Courtesy of the John I. Koivula inclusion collection.

Gems & Gemology, Vol. 61, No. 4, pp. 400–406.

Figure 2. A Russian emerald carving, approximately 41 × 25 mm, of a woman holding blooming flowers, reportedly fashioned by Michael Peuster. Photo by Ronnakorn Manorotkul; courtesy of Tsarina Jewels.

examples. It was a delightful coincidence to find that the inclusion scene in this stone echoed the floral motif carved into its exterior.

E. Billie Hughes
Lotus Gemology, Bangkok

Figure 4. Near-colorless heulandite crystals resembling worms in an Ethiopian opal exhibiting play-of-color. Photomicrograph by Bawornluk Keeratithanarut; field of view 2.88 mm.

"Worms" in Opal

Opal is an amorphous gemstone known for its unique play-of-color phenomenon. Additionally, opal hosts a wide range of mineral inclusions. Recently, an interesting inclusion was observed in a 22.96 ct Ethiopian opal. Standard gemological testing and Fourier-transform infrared spectroscopy confirmed the opal as natural and untreated. Microscopic examination revealed the presence of near-colorless crystal inclusions (figure 4), matching heulandite of the zeolite group when identified by Raman spectroscopy. These inclusions exhibited a distinctive morphology, resembling worms with elongated, segmented bodies. In some areas, the inclusions appeared twisted, further enhancing their serpentine illusion.

Bawornluk Keeratithanarut
GIA, Bangkok

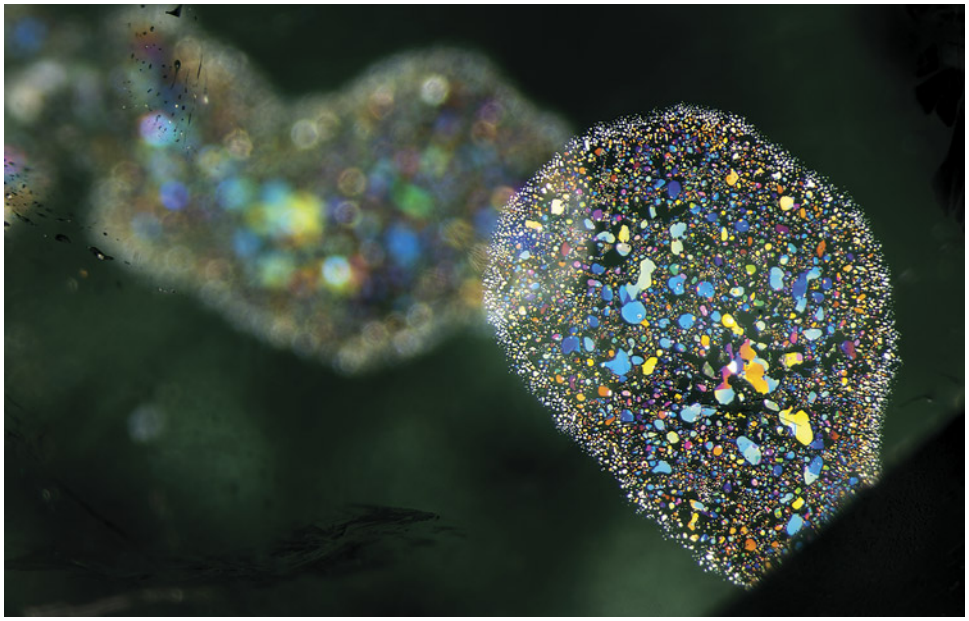

Figure 3. Like an artist's palette, clusters of stacked thin films create a bouquet of color inside this Russian emerald. Photomicrograph by E. Billie Hughes; field of view 5.4 mm.

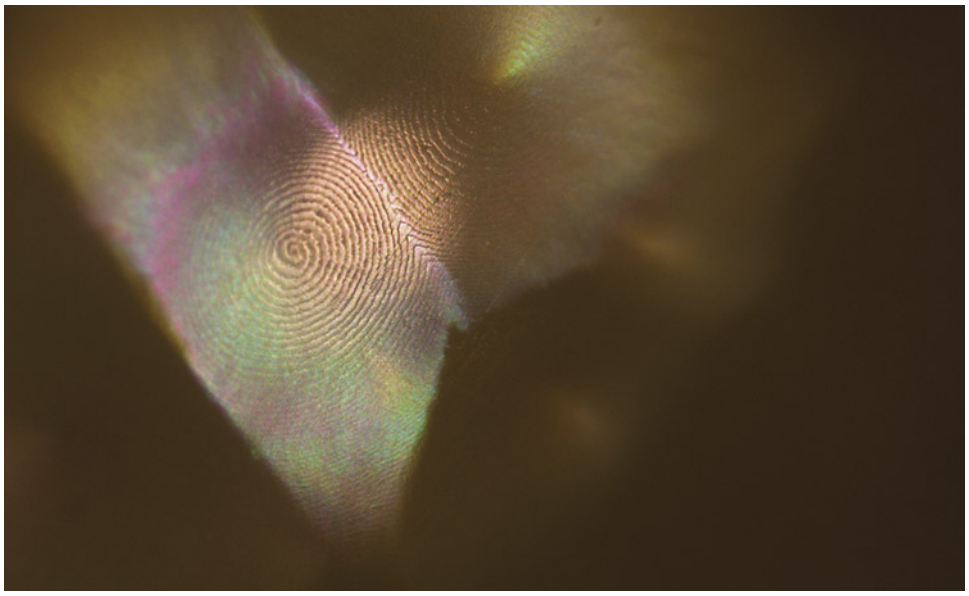

Figure 5. Spiral pattern of nacre platelets observed in each polygon of the mosaic pattern. Photomicrograph by Nishka Vaz; field of view 0.5 mm.

Fingerprint Pattern on a "Hammered" Pearl's Surface

Among a parcel of saltwater natural and cultured pearls, a white near-button, non-bead cultured pearl, weighing 3.18 ct and measuring 8.06 × 7.81 × 6.57 mm, recently stood out due to its unusual external appearance. The pearl's surface exhibited a mosaic of indentations surrounded by ridges, visually similar to the hammered effect seen on metal ornaments (Summer 2024 *G&G* Micro-World, pp. 228–229). Bright spots of light reflected from the center of each polygonal subsurface indentation. Each indentation displayed a spiral pattern of nacre platelets resembling a human fingerprint, with the center of the spiral aligning with the center of each polygon (figure 5). The strong iridescence produced by the nacre platelets was complemented by shimmering flashes of light within the mosaic, which seemed to float just beneath the pearl's surface. This subtle optical effect combined with the beautifully symmetrical nacre spirals makes this pearl noteworthy.

Nishka Vaz and Abeer Al-Alawi
GIA, Mumbai

Hanabi in a Conch Pearl

Conch pearls are often appreciated for their pleasing pink bodycolor and striking flame structures. These pearls can exhibit a variety of flame patterns, from long and narrow to short and broad flames. Recently, the author encountered a conch pearl that displayed truly captivating patterns.

The pink oval conch pearl weighed 5.95 ct and measured 10.68 × 9.22 × 7.38 mm. At first glance, eye-visible flame structures were observed. Microscopic examination under fiber-optic light revealed a fascinating discovery of firework-like flame patterns (figure 6). The combination of these patterns and the warm pink bodycolor of the pearl was reminiscent of *hanabi*, the Japanese word for "fireworks," which illuminate the sky every summer at festivals in Japan.

Flame structures can be explained by the interaction between light and aragonite lamellae microstructures of the pearl (H.A. Hänni, "Explaining the flame structure of non-nacreous pearls," *Australian Gemmologist*, Vol. 24, No. 4, 2010, pp. 85–88). While it is rather common to find flame structures on conch pearls, the patterns exhibited by this specimen were remarkable.

Hazel "Wing Kiu" Fan
GIA, Hong Kong

Figure 6. A 5.95 ct pink oval conch pearl exhibiting firework-like flame patterns. Photomicrograph by Hazel "Wing Kiu" Fan; field of view 5.98 mm.

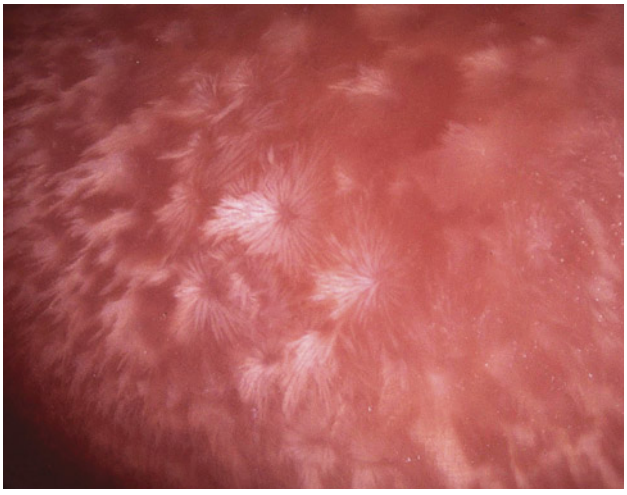

Figure 7. Fibrous mannardite crystals in quartz. Photomicrograph by Liyan He; field of view 2.98 mm.

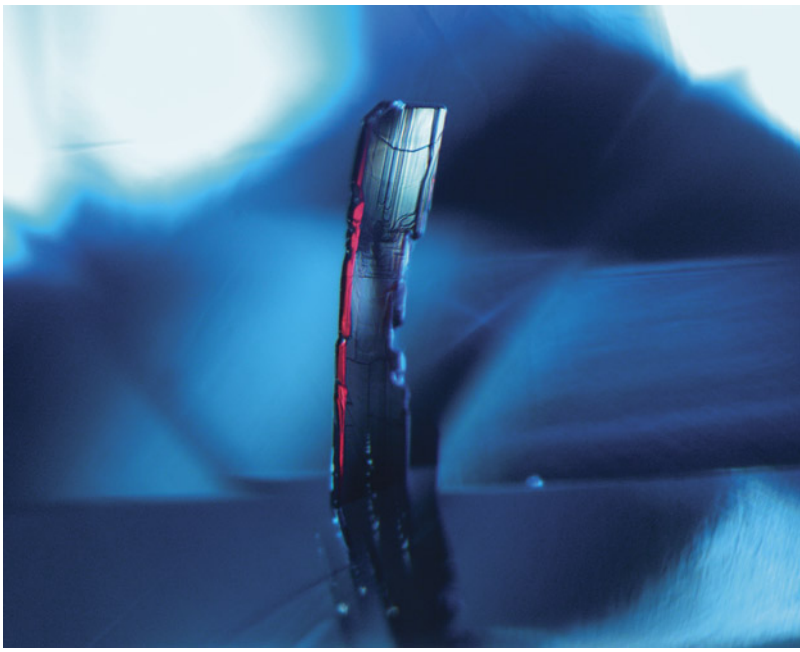

Figure 8. Red prismatic tantalite breaking the surface of a greenish blue sapphire. Photomicrograph by Axle Estrella; field of view 1.93 mm.

Mannardite in Quartz

Recently, the authors investigated a set of three colorless quartz samples, each exhibiting distinctive black fibrous inclusions. Microscopic observation revealed that the metallic opaque crystals were often arranged in parallel or radial formations (figure 7). These inclusions were identified by Raman spectroscopy as the rare mineral mannardite ($Ba(Ti^{4+}_{6}V^{3+}_{2})O_{16}$). Mannardite is a member of the cryptomelane group (hollandite) and is found in Russia, Northwest Kazakhstan, and South China, with these inclusions typically ranging from 15 to 50 μm in width.

This discovery offers new insights into low-temperature hydrothermal mineralization processes, as the coexistence of mannardite with quartz suggests formation under specific redox conditions (X. Fu et al., "Mineralogy and trace element geochemistry of the early Cambrian black shale-hosted Zhongcun vanadium deposit, southern Qinling, China," *Ore Geology Reviews*, Vol. 155, 2023, article no. 105371). These findings contribute to understanding vanadium-rich mineral paragenesis in quartz-bearing systems and highlight Raman spectroscopy's critical role in nondestructive mineral identification at the micrometer scale.

Liyan He
Guangdong Gemstones & Precious Metals Testing Center
Guangzhou, China
Wingtak Lui
Min De Minerals & Gem Research Co. Ltd.
Nanjing, China

Dark Red Tantalite Crystal in Greenish Blue Sapphire

The authors recently examined a 1.80 ct greenish blue sapphire and were surprised to observe a dark red internal protuberance jutting inward from the surface of the pavilion (figure 8). The prismatic inclusion was identified as manganotantalite ($(Mn,Fe)(Ta_2O_6)$; a manganese-enriched iron-tantalum oxide) using Raman spectroscopy, consistent with its red bodycolor. This mineral displayed a blunt termination and etched pinacoidal surfaces. Laser ablation–inductively coupled plasma–mass spectrometry analysis showed that the host sapphire had iron levels of up to 1900 ppma. With a spectroscope, a strong broad absorption around 840–880 nm was observed. These observations are consistent with known occurrences of tantalite in sapphire hosts from basaltic-related origins (S. Promwongnan and C. Sutthirat, "Mineral inclusions in ruby and sapphire from the Bo Welu gem deposit in Chanthaburi, Thailand," Fall 2019 *G&G*, pp. 354–369).

While tantalite itself is not uncommon in sapphires of this type, this inclusion was notable due to its interesting morphology and attractive dark red color, attributed to the presence of manganese, which contrasted with the greenish blue stone (O.I. Lee and E.T. Wherry, "Manganotantalite from Amelia, Virginia," *American Mineralogist*, Vol. 4, No. 7, 1919, pp. 80–83).

Axle Estrella and Joseph Hukins
GIA, New York

Figure 9. Natural 1.36 ct scapolite with saturated blue spindle-shaped lazurite inclusions. Photos by Lhapsin Nillapat (left) and Chinnaphat Buntem; field of view 2.90 mm (right).

Spindle-Shaped Lazurite Inclusions in Scapolite

The author recently examined a 1.36 ct near-colorless, transparent scapolite gemstone containing an abundance of eye-visible vivid blue inclusions (figure 9). These spindle-shaped inclusions were identified as lazurite by Raman spectroscopy. Under microscopic observation, the well-defined symmetrical shapes, sharp boundaries, and intensely saturated blue color of the inclusions were readily observed due to the high clarity of the scapolite host. Lazurite within scapolite is rare and has been reported mainly from the Sar-e-Sang mines in Badakhshan, Afghanistan (S.W. Faryad, "Metamorphic conditions and fluid compositions of scapolite-bearing rocks from the lapis lazuli deposit at Sare Sang, Afghanistan," *Journal of Petrology*, Vol. 43, No. 4, 2002, pp. 725–747).

Chinnaphat Buntem
GIA, Bangkok

Metal Sulfide in Spinel

Recently, a 3.14 ct pink spinel was submitted to the Lotus Gemology laboratory, with encouragement from the owner to examine its inclusions. When viewed under the microscope, the spinel did not disappoint. Suspended within was a richly textured, opaque metallic crystal (figure 10). Although attempts were made to identify the inclusion using micro-Raman spectroscopy, its identity remained inconclusive. However, based on the crystal's appearance, it was likely a metal sulfide. Similar inclusions in spinel have been reported as pyrite (E.B. Hughes et al., "Spinel inclusions: An exercise in aesthetics," *InColor*, No. 43, 2019, pp. 66–73; N. Renfro et al., "Micro-features of spinel," Spring 2021 *G&G*, pp. 46–49).

E. Billie Hughes
Lotus Gemology, Bangkok

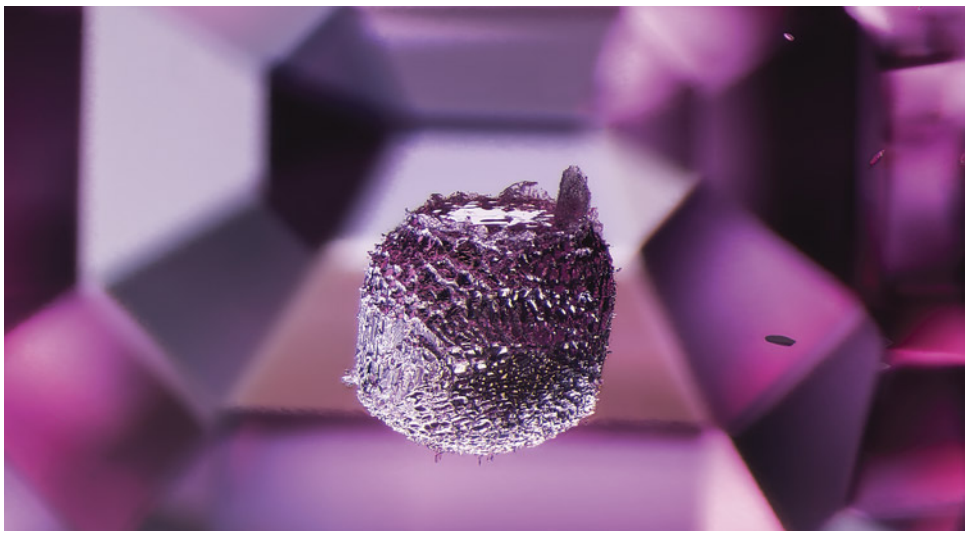

Figure 10. A strikingly textured crystal, likely a metal sulfide, is suspended within a pink spinel; viewed under darkfield and diffuse fiber-optic lighting. The step-cut facets on the stone's pavilion provide a sense of depth to the image. Photomicrograph by E. Billie Hughes; field of view 3.4 mm.

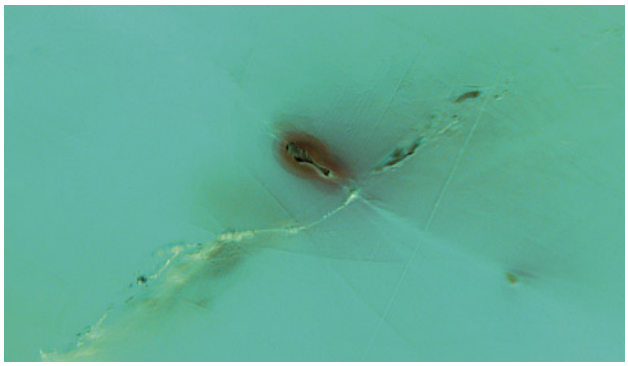

Figure 11. Top view of an altered etch tube in tourmaline resembling a drumstick of a chicken. Photomicrograph by Jamie Price; field of view 1.16 mm.

Whimsical Growth Tubes in Tourmaline

Crystals formed within pegmatitic environments are exposed to hydrothermal fluids that may alter the mineral both externally and internally via fractures or etch channels. The hydrothermal fluids sometimes contain radioactive elements such as uranium, thorium, and radium, which can cause alterations to the host crystal. Evidence of radiation damage is often found in diamond and in copper-bearing tourmaline, referred to as "radiation stains" and "pink sleeves," respectively (J.I. Koivula et al., "Solution-generated pink color surrounding growth tubes and cracks in blue to blue-green copper-bearing tourmalines from Mozambique," Spring 2009 *G&G*, pp. 44–47).

Recently, the author examined a 37.09 ct copper-bearing tourmaline containing many growth tubes that had been altered by radioactive hydrothermal fluids, two of which were intriguing. When viewed directly down the length of the etch tubes, one area resembled a drumstick of a chicken (center of figure 11), while another area looked like the face of a bird with a fuzzy tuft (figure 12).

Jamie Price
GIA, Carlsbad

Figure 12. Top view of an altered etch tube in tourmaline resembling the face of a bird with a fuzzy tuft. Photomicrograph by Jamie Price; field of view 1.48 mm.

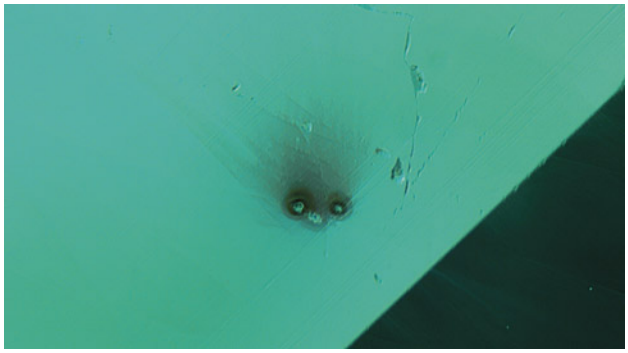

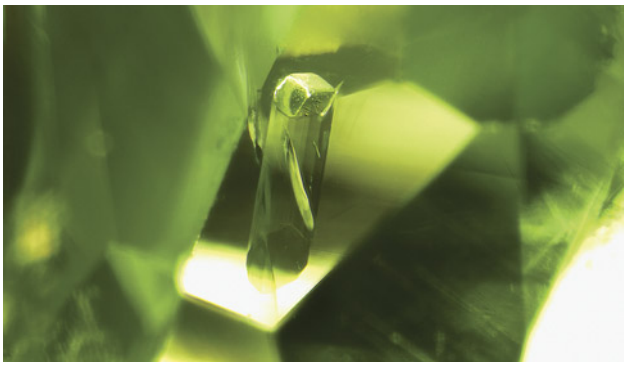

Figure 13. A euhedral tourmaline crystal in a tourmaline host. Photomicrograph by Hikaru Sato; field of view 1.95 mm.

Tourmaline in Tourmaline

The author recently examined a 0.16 ct transparent oval modified brilliant tourmaline containing an included euhedral crystal (figure 13). The inclusion, identified by Raman spectroscopy as tourmaline, displayed a rolled trigonal prism with blunt terminations and associated stress fractures. Tourmaline inclusions in tourmaline have been previously documented (N. Renfro et al., "Micro-features of tourmaline," Summer 2024 *G&G*, pp. 208–210); however, it is rare to see such a perfectly shaped crystal inclusion.

Hikaru Sato
GIA, Tokyo

Quarterly Crystal: β-Quartz Morphology in Beryl

The specimen shown in figure 14, weighing 80.60 ct and measuring approximately 28 × 24 × 22 mm, consists of a

Figure 14. A sharply defined inclusion of α-quartz with β-quartz form is observed within beryl. Photo by Harold Moritz.

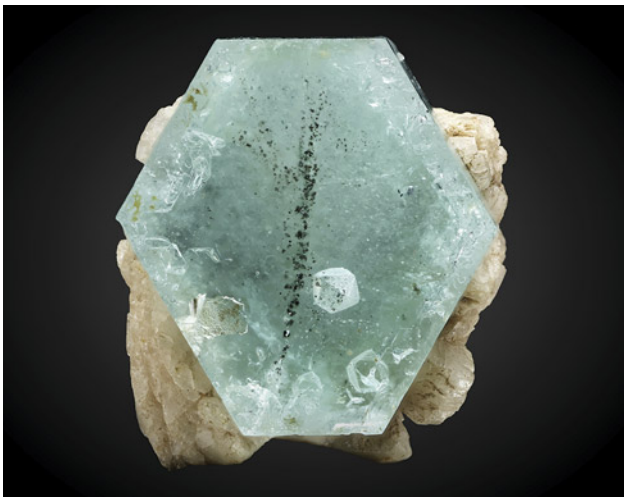

sharp, well-formed aquamarine beryl crystal grown on microcline feldspar crystals. The sample is from Pakistan's Shigar Valley in the Skardu district of Gilgit-Baltistan.

Microscopic examination revealed a single, sharply defined inclusion approximately 3 mm in length (figure 15). The strikingly short bipyramidal morphology is characteristic of β-quartz, the high-temperature polymorph of silicon dioxide, which usually transitions to α-quartz upon cooling below ~570°C (W.L. Bragg and R.E. Gibbs, "The structure of α and β quartz," *Proceedings of the Royal Society of London*. Series A, Vol. 109, No. 751, 1925, pp. 405–427). That transition typically destroys the original crystal shape, making preserved β-quartz morphology exceedingly rare in nature.

In this case, it appears that rapid encapsulation within the growing beryl may have frozen the morphology in place before the reconstructive transition could alter the form. While the inclusion is α-quartz in structure today, as confirmed by Raman spectroscopy, its preserved β-quartz–like shape raises intriguing questions about formation conditions and cooling rates. A literature search failed to reveal any other examples of the β-quartz form preserved within beryl.

Russell E. Behnke
Meriden, Connecticut

Figure 15. The 3 mm β-quartz inclusion pseudomorphed to α-quartz in the beryl host. Photomicrograph by Harold Moritz; field of view 9.00 mm.